

FACULTY OF ENGINEERING  
ALEXANDRIA UNIVERSITYAlexandria University  
**Alexandria Engineering Journal**[www.elsevier.com/locate/aej](http://www.elsevier.com/locate/aej)  
[www.sciencedirect.com](http://www.sciencedirect.com)

## ORIGINAL ARTICLE

# Enhancing the accuracy of GPS point positioning by converting the single frequency data to dual frequency data

Aly M. El-naggar

*Transportation Department, Faculty of Engineering, Alexandria University, Egypt*

Received 6 December 2010; accepted 5 March 2011

Available online 5 October 2011

**KEYWORDS**GPS signal;  
Single frequency;  
Dual frequency;  
TEC

**Abstract** The global positioning system (GPS) has been used to support a wide variety of applications, such as high-accuracy positioning and navigation. Differential GPS techniques can largely eliminate common-mode errors between the reference and the rover GPS stations resulting from ionospheric and tropospheric refraction and delays, satellite and receiver clock biases, and orbital errors [1]. The ionospheric delay in the propagation of global positioning system (GPS) signals is one of the main sources of error in GPS precise positioning and navigation. A dual-frequency GPS receiver can eliminate (to the first order) the ionospheric delay through a linear combination of the L1 and L2 observations [2]. The most significant effect of ionospheric delay appear in case of using single frequency data. In this paper the single frequency data of concerned station are converted to dual frequency data by employing dual frequency data from 11 regional GPS stations distributed around it. Total electron content (TEC) was calculated at every GPS station to produce the mathematical model of TEC which is a function of latitude ( $\Phi$ ) and longitude ( $\lambda$ ). By using this mathematical model the values of TEC and L2 can be predicted at the single frequency GPS station for each satellite, after that the comparison between predicted and observation values of TEC and L2 was performed. The estimation method and test results of the proposed method indicates that the difference between predicted and observation values is very small.

© 2011 Faculty of Engineering, Alexandria University. Production and hosting by Elsevier B.V.  
All rights reserved.

E-mail address: [aly\\_m\\_gad@yahoo.com](mailto:aly_m_gad@yahoo.com)1110-0168 © 2011 Faculty of Engineering, Alexandria University.  
Production and hosting by Elsevier B.V. All rights reserved.

Peer review under responsibility of Faculty of Engineering, Alexandria University.

doi:10.1016/j.aej.2011.03.003



Production and hosting by Elsevier

**1. Introduction**

Global positioning system (GPS) measurements can be corrupted by several error sources. These errors are categorized as biases and random errors, i.e. ionosphere, troposphere, satellite clock, receiver clock offsets, receiver noise, and multipath. Differential GPS (DGPS) provides users with corrections to remove the correlated bias terms between receivers [3].

After the turn-off of the selective availability (SA), the ionosphere effect has become the largest error source in GPS positioning and navigation. For high precision GPS positioning, the ionosphere effect must be estimated so that a correction can be made to eliminate it from the GPS observations [4].

When radio waves propagate through the ionosphere they suffer an extra time delay. This time delay is a function of the total electron content (TEC) of the ionosphere. Since the ionosphere acts as a dispersive medium to GPS signals, dual-frequency (L1 at 1575.42 MHz, L2 at 1227.60 MHz) GPS receivers can eliminate (albeit to the first order) ionospheric delay through a linear combination of L1 and L2 observations [2].

The codes transmitted by GPS satellites at the two L-band frequencies (L1–L2) are carefully synchronized so that they are broadcast simultaneously. Absolute simultaneity is not possible, however, so the time difference between the transmitted times at the two frequencies is called the satellite L1/L2 differential delay or satellite differential delay. Each GPS satellite has a unique satellite differential delay. Differential frequency delays may also be present in GPS receivers. These are called the receiver L1/L2 differential delay or receiver differential delay, because the L1 and L2 signals must travel through different hardware paths or electronic circuitry inside the receiver. Each GPS receiver has its individual receiver differential delay. Both the satellite and receiver differential delays introduce error in the measurement of TEC. The paper is organized as follows. Section 2 discusses the ionosphere, ionospheric delays, and ionospheric modeling. While the description of data used is presented in Section 3. Ionospheric delays are derived from GPS dual-frequency observations, and numerical results and performance analysis are provided in Section 4. Conclusions are given in Section 5.

## 2. Ionosphere

The ionosphere is a shell of electrons and electrically charged atoms and molecules that surrounds the Earth, stretching from a height of about 50 km to more than 1000 km. It owes its existence primarily to ultraviolet radiation from the sun.

The lowest part of the Earth's atmosphere, the troposphere extends from the surface to about 10 km (6 miles). Above 10 km is the stratosphere, followed by the mesosphere. In the stratosphere incoming solar radiation creates the ozone layer. At heights of above 80 km (50 miles), in the thermosphere, the atmosphere is so thin that free electrons can exist for short periods of time before they are captured by a nearby positive ion. The number of these free electrons is sufficient to affect radio propagation. This portion of the atmosphere is ionized and contains a plasma which is referred to as the ionosphere. In a plasma, the negative free electrons and the positive ions are attracted to each other by the electromagnetic force, but they are too energetic to stay fixed together in an electrically neutral molecule.

Ionization depends primarily on the Sun and its activity. The amount of ionization in the ionosphere varies greatly with the amount of radiation received from the sun. Thus there is a diurnal (time of day) effect and a seasonal effect. The local winter hemisphere is tipped away from the Sun, thus there is less received solar radiation. The activity of the sun is associated with the sunspot cycle, with more radiation occurring with more sunspots. Radiation received also varies with

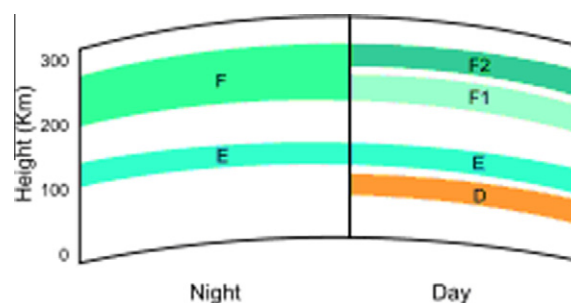


Figure 1 Ionospheric layers.

geographical location (polar, auroral zones, mid-latitudes, and equatorial regions). There are also mechanisms that disturb the ionosphere and decrease the ionization. There are disturbances such as solar flares and the associated release of charged particles into the solar wind which reaches the Earth and interacts with its geomagnetic field [5].

The ionosphere is a dispersive and anisotropic medium for radio waves. Taking advantage of the dispersive nature of the ionosphere, the first-order ionospheric term may fully be eliminated by differencing the signal at two different frequencies.

Several authors reveal that higher-order ionospheric errors may vary from few millimeters to several centimeters depending on satellite elevation and azimuth angles, and the ionospheric and geomagnetic conditions. Therefore, if millimeter level accuracy is needed in precise point positioning (PPP), higher-order errors cannot be ignored. The second and third order errors are typically  $\sim 0$  to 2 cm and  $\sim 0$  to 2 mm at zenith respectively [6].

### 2.1. The ionospheric layers

At night the F layer is the only layer of significant ionization present, while the ionization in the E and D layers is extremely low. During the day, the D and E layers become much more heavily ionized, as does the F layer, which develops an additional, weaker region of ionization known as the F1 layer. The F2 layer persists by day and night and is the region mainly responsible for the refraction of radio waves (Fig. 1) [5].

#### 2.1.1. D layer

The D layer is the innermost layer, 60–90 km above the surface of the Earth. Ionization here is due to Lyman series-alpha hydrogen radiation at a wavelength of 121.5 nm ionizing nitric oxide (NO). In addition, with high solar activity hard X-rays (wavelength  $< 1$  nm) may ionize ( $N_2$ ,  $O_2$ ). During the night cosmic rays produce a residual amount of ionization. Recombination is high in the D layer, the net ionization effect is low, but loss of wave energy is great due to frequent collisions of the electrons (about 10 collisions every msec). As a result high-frequency (HF) radio waves are not reflected by the D layer but suffer loss of energy therein. This is the main reason for absorption of HF radio waves, particularly at 10 MHz and below, with progressively smaller absorption as the frequency gets higher. The absorption is small at night and greatest about midday. The layer reduces greatly after sunset; a small part remains due to galactic cosmic rays.

During solar proton events, ionization can reach unusually high levels in the D-region over high and polar latitudes. Such

very rare events are known as Polar Cap Absorption (or PCA) events, because the increased ionization significantly enhances the absorption of radio signals passing through the region.

#### 2.1.2. *E layer*

The E layer is the middle layer, 90–120 km above the surface of the Earth. Ionization is due to soft X-ray (1–10 nm) and far ultraviolet (UV) solar radiation ionization of molecular oxygen (O<sub>2</sub>). Normally, at oblique incidence, this layer can only reflect radio waves having frequencies lower than about 10 MHz and may contribute a bit to absorption on frequencies above. However during intense Sporadic E events the Es layer can reflect frequencies up to 50 MHz and higher. The vertical structure of the E layer is primarily determined by the competing effects of ionization and recombination. At night the E layer rapidly disappears because the primary source of ionization is no longer present. After sunset an increase in the height of the E layer maximum increases the range to which radio waves can travel by reflection from the layer. This region is also known as the Kennelly–Heaviside layer or simply the Heaviside layer. Its existence was predicted in 1902 independently and almost simultaneously by the American electrical engineer Arthur Edwin Kennelly (1861–1939) and the British physicist Oliver Heaviside (1850–1925).

#### 2.1.3. *Es*

The Es layer (sporadic E-layer) is characterized by small, thin clouds of intense ionization, which can support reflection of radio waves; rarely up to 225 MHz. Sporadic-E events may last for just a few minutes to several hours. Sporadic E propagation makes radio amateurs very excited, as propagation paths that are generally unreachable can open up. There are multiple causes of sporadic-E that are still being pursued by researchers. This propagation occurs most frequently during the summer months when high signal levels may be reached.

#### 2.1.4. *F layer*

The F layer or region, also known as the Appleton layer extends from about 200 km to more than 500 km above the surface of Earth. It is the densest point of the ionosphere, which implies signals penetrating this layer will escape into space. Beyond this layer is the topside ionosphere. Here extreme ultraviolet (UV, 10–100 nm) solar radiation ionizes atomic oxygen. The F layer consists of one layer at night, but during the day, a deformation often forms in the profile that is labeled F1. The F2 layer remains by day and night responsible for most sky wave propagation of radio waves, facilitating high frequency (HF, or shortwave) radio communications over long distances. From 1972 to 1975 NASA launched the AEROS and AEROS B satellites to study the F region [5].

### 2.2. *Ionospheric delays*

The ionosphere is the region of ionized plasma extending 80–1200 km above the Earth's surface and forms the transition region between the neutral atmosphere and the fully ionized magnetospheric plasma. Free electrons and ions are produced during interaction of extreme ultra violet (EUV) and X-ray radiation with upper atmosphere neutral gas. Ionospheric activity is subject to regular diurnal, seasonal, and solar cycle variation as well as irregular geomagnetic activity caused by solar storms, traveling ionospheric disturbances, and scintilla-

tion. Diurnal electron density peaks at 2 h past local noon, and solar cycle variation during increased sunspot activity associated with 11 year solar variations. During nighttime, the D- and E-layers disappear and the F1 and F2 layers combine to form the F layer. The maximum electron density occurs in the F2 layer. The ionosphere significantly affects terrestrial-based radio communication and attenuates high frequency wave propagating through it. Its effect on radio waves of astronomical origin in the bandwidth 70–20 GHz includes phase delay, phase jitter, attenuation, refraction, scintillation, and Faraday rotation; left polarized rotation. These phenomena are proportional to the total electron content (TEC) of the plasma along the signal path. Ionospheric errors on signals received from GPS satellites signals constitute the largest contributor to errors in position fix by single-frequency GPS receivers. These phenomena are more pronounced during periods of severe solar activity such as geomagnetic storms. The Satellite Based Augmentation Systems (SBAS) such as the American Wide Area Augmentation System (WAAS) and the European Geostationary Navigation Overlay Service (EGNOS) have, in part, been developed to supply near real-time ionospheric correction parameters to GPS users for precision navigation and surveying applications [7].

For any radiometric space technique, such as those utilizing global navigation satellite systems (GNSS), it is necessary to account for the propagation delay caused by the neutral atmosphere. Because of the nature of the neutral atmosphere, which is composed mainly of gases including water vapor, a radio signal is refracted when passing through the atmosphere, which means its speed changes (the signal travels more slowly than the vacuum speed of light) as does its path (the signal doesn't travel in a straight line between the signal source and the receiver). Due to these changes in speed and direction, it takes longer for the signal to reach the receiver's antenna than if it was traveling through a vacuum. This difference in time, which can also be represented in units of length, is the neutral atmosphere propagation delay. The magnitude of this delay depends on the profile of the refractive index along the signal's path, which is determined by the values of total atmospheric pressure, temperature, and the partial pressure of water vapor [4].

The ionospheric effect is an important error source in GPS measuring. The amount of the ionospheric delay or advance of the GPS signal can vary from a few meters to more than 20 m within one day. Generally, it is difficult to model the ionospheric effects due to complicated physical interactions among the geomagnetic field and solar activities. However, the ionosphere is a dispersive medium, i.e., the ionospheric effect is frequency dependent. Using this property, the GPS system is designed with several working frequencies, so that ionospheric effects can be measured or corrected [8].

One of the largest error sources in a single-frequency GPS solution is due to the ionosphere which both slows and refracts GPS signals as they propagate through it. This unknown propagation delay is highly variable and dependent upon several factors, such as: time of day, latitude, solar activity and season. The effect is proportional to the total electron content (TEC), the line integral of the ionospheric electron density [9].

### 2.3. *Ionospheric model*

An ionospheric model is a mathematical description of the ionosphere as a function of location, altitude, day of year, phase

of the sun spot cycle and geomagnetic activity. Geophysically, the state of the ionospheric plasma may be described by four parameters: electron density, electron and ion temperature and, since several species of ions are present, ionic composition. Radio propagation depends uniquely on electron density. Models are usually expressed as computer programs. The model may be based on basic physics of the interactions of the ions and electrons with the neutral atmosphere and sun light, or it may be a statistical description based on a large number of observations or a combination of physics and observations. One of the most widely used models is the International Reference Ionosphere (IRI), which is based on data and specifies the four parameters just mentioned. The IRI is an international project sponsored by the Committee on Space Research (COSPAR) and the International Union of Radio Science (URSI). IRI is updated yearly. IRI is accurate in describing the variation of the electron density from bottom of the ionosphere to the altitude of maximum density than in describing the total electron content (TEC) [5].

### 3. Data used

Performance analysis was conducted using data from regional GPS reference networks. The data from Oregon Real-time Network GPS reference network (ORGN) has been used to evaluate the estimation method of TEC and L2 signal. The used stations of (ORGN) network (Fig. 2) consist of 12 continuously operating GPS. Oregon Real-time GPS Network, including network status, products and services, support information, and contacts is located at website [www.theorgn.net](http://www.theorgn.net). The coordinates for active and used ORGN stations are listed below in Table 1.

### 4. TEC and L2 prediction using GPS measurements

The ionosphere affects the electromagnetic waves that pass through it by inducing an additional transmission time delay. The magnitude of this effect is determined by the amount of total electron content (TEC) and the frequency of electromagnetic waves. Under normal solar activity conditions, this influence on GPS signals is usually in the range from a few meters

**Table 1** Oregon Real-time Network (ORGN) coordinates.

Station ID	Latitude $\Phi$ (N)			Longitude $\lambda$ (W)		
	<i>d</i>	<i>M</i>	<i>s</i>	<i>d</i>	<i>M</i>	<i>s</i>
ARLN	45	42	30.6051	120	10	59.71137
ASHL	42	10	51.62383	122	40	12.5521
CHEM	43	13	27.6913	121	47	8.940166
CTPT	42	22	37.34693	122	53	38.19423
ENTR	45	25	53.61965	117	17	17.03843
GTPS	42	26	5.426762	123	17	50.50984
ONAB	44	30	51.71934	124	4	28.20139
PKDL	45	31	7.016973	121	33	49.18925
PSPT	42	45	18.41405	122	29	22.1643
SEAS	45	59	3.912371	123	55	20.66374
TDLS	45	36	28.87746	121	7	46.16529
TILL	45	27	19.57444	123	49	50.70493

to tens of meters but it could reach more than 100 m during severe ionosphere storms [4].

In particular for this paper, the dual-frequency nature of the GPS signal allows one to extract ionospheric total electron content (TEC) (i.e. integrated free electron density) information along the line-of-sight between the satellite and receiver [10].

A radio signal propagating through the ionosphere experiences a group delay and phase advance due to the ionosphere's dispersive nature. This delay/advance is proportional to the total electron content (TEC) along the signal path and inversely proportional to the square of the carrier frequency.

$$\Delta_{ph}^{iono} = -\frac{40.3}{f^2} \text{TEC} \text{ and } \Delta_{gr}^{iono} = \frac{40.3}{f^2} \text{TEC}$$

TEC is quantified from GPS measurements by a linear combination of the measured pseudo range and phase observables registered by the receiver on two carrier frequencies ( $f^1 = 1575.4$  MHz and  $f^2 = 1227.6$  MHz).

TEC is measured in TEC units with  $1 \text{ TECU} = 10^{16} \text{ em}^{-2}$ . Measured pseudo range ( $P$ ), constitute a combination of the geometric range, ( $\rho$ ), speed of light in a vacuum ( $c$ ), ionospheric range error ( $\Delta\rho_{ion}$ ), tropospheric range error ( $\Delta\rho_{trop}$ ),

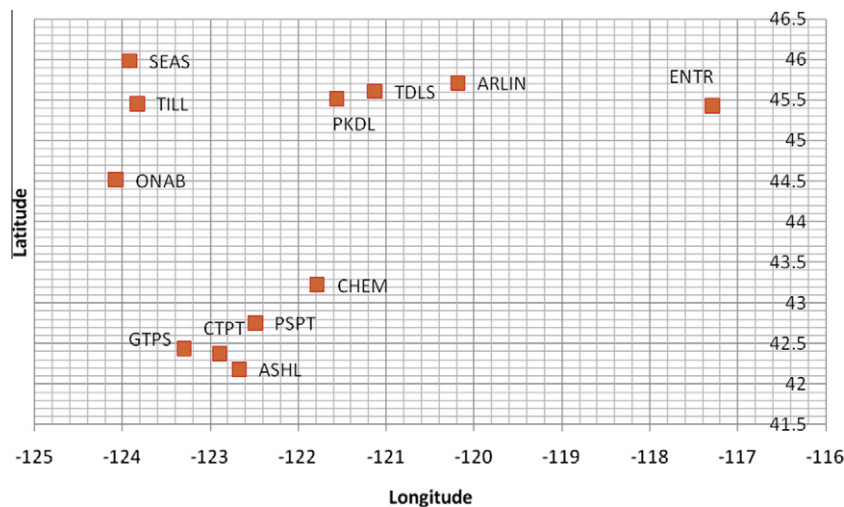


**Figure 2** Oregon Real-time Network (ORGN) reference stations.

satellite and receiver biases,  $b_S$  and  $b_R$ , multipath and other errors ( $\varepsilon$ ):

$$P = \rho + \Delta\rho_{ion} + \Delta\rho_{trop} + c(\Delta t_c^S - \Delta t_c^R) + c(b_S + b_R) + \varepsilon$$

Likewise the measured phase can be expressed as

$$L = \rho - \Delta\rho_{ion} + \Delta\rho_{trop} + c(\Delta t_c^S - \Delta t_c^R) + \lambda B + E$$

where  $\lambda$  is the carrier wavelength and  $B$  an unknown integer ambiguity offset. Code-based TEC is calculated from the difference between the two observed pseudo ranges.

$$P_4 = P_2 - P_1 = \left(\frac{1}{f_2} - \frac{1}{f_1}\right) \cdot \alpha \cdot TEC_P, \quad \alpha = 40.3 \times 10^{16}$$

and

$$L_4 = L_1 \frac{c}{f_1} - L_2 \frac{c}{f_2} = \left(\frac{1}{f_2} - \frac{1}{f_1}\right) \cdot \alpha \cdot TEC_L$$

Therefore it can be estimate the L2 as follows

$$L_2 = \frac{f_2}{c} \left[ L_1 \frac{c}{f_1} - \left(\frac{1}{f_2} - \frac{1}{f_1}\right) \cdot \alpha \cdot TEC_L \right]$$

Code-based TEC ( $TEC_P$ ) is noisier than phase-based TEC ( $TEC_L$ ), largely due to multipath, but the latter suffers an unknown integer ambiguity offset and is subject to cycle slips associated with rapid ionospheric scintillations. The resultant product is the GPS-derived slant TEC along the signal path between satellite and receiver [7].

If a second frequency is used, TEC can easily be determined due to the dispersive behavior of the ionosphere:

$$TEC = \frac{c}{40.3} \left(\frac{1}{f_1} - \frac{1}{f_2}\right) \cdot \delta\tau_{ff_2}$$

where  $\delta\tau_{ff_2}$  is the travel time difference between both radio signals.

The TEC values are calculated at each station and the contour map was drawn to produce the TEC contour map (Fig. 3). This map shows that well and equal spaced contour line due to strong correlation between TEC values for all GPS stations.

#### 4.1. Modeling the ionosphere using the second order polynomial

A dual frequency GPS receiver measures pseudo-range and carrier phases at L1/L2 and its observables are used to compute TEC for each tracked satellite at each GPS station.

The second ordered polynomial for estimation the TEC at any point of  $\lambda$  and  $\Phi$  can be expressed as follows

$$TEC(\lambda, \Phi) = a_0 + a_1\lambda + a_2\Phi + a_3\lambda\Phi + a_4\lambda^2 + a_5\Phi^2$$

This model can be expressed as

$$V = A \cdot X + L$$

where  $V$  = Vector of residuals,  $A$  = The coordinates of GPS stations,  $X = a_0, a_1, \dots, a_5$  Are known coefficients, which will be solved using the least square techniques, and  $L$  = The TEC value at each GPS station.

The normal equations become

$$(A^T \cdot A) \cdot X = A^T \cdot L$$

or

$$N \cdot X = A^T \cdot L$$

The least square will solve these equations by minimizing the sum of the squares of the residuals, and the solution will be in the form:

$$X = N^{-1} \cdot A^T \cdot L$$

Once the model coefficients were obtained, the obtained model parameters are used to calculate the TEC value for the concerned station for each satellite. If the model derived can be compared to its directly measured value from the concerned station GPS observations, the comparison results are provided in Table 2 where the differences indicated an agreement between the model-derived estimates and the direct measurements at the level of 0.00237%.

Shown in Table 2 are the difference error estimates in percentage calculated using the following equation:

$$DE = \frac{TEC_{calculated} - TEC_{actual}}{TEC_{calculated}} \cdot 100$$

Once the TEC values are calculated at check GPS station (TDLS GPS station), it can be estimate the L2 as follows

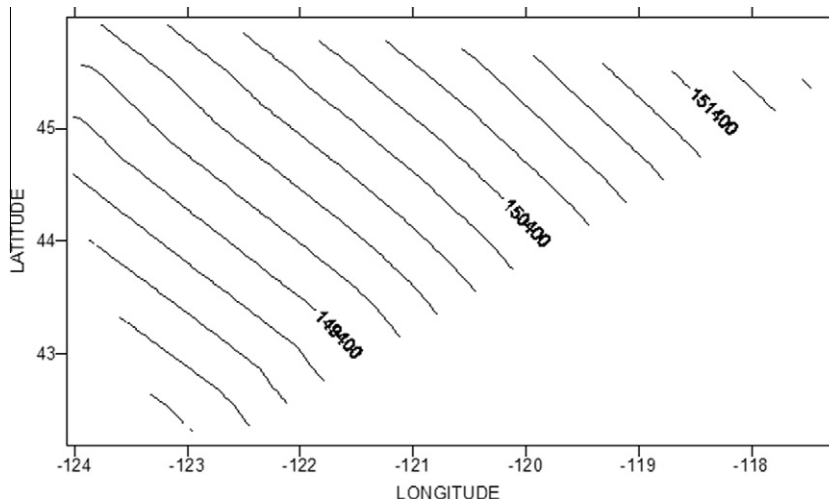


Figure 3 TEC contour map.

**Table 2** Actual and estimated values of TEC for each satellite.

Satellite #	S3	S6	S9	S11	S14	S18	S19	S22
(TEC)calculated	150558.8	151087	148731.7	157578.9	134072.6	146428.8	144062.4	134192.2
(TEC)actual	150554.8	151067.3	148699.2	157618.5	134075.7	146396.7	144057.7	134223.8
Difference error %(DE)	0.002625	0.01304	0.021836	-0.0251	-0.00237	0.021919	0.003239	-0.02358

**Table 3** Actual and estimated values of L2 for each satellite.

Satellite #	(L2) Calculated	(L2) Actual	Difference error %(DE)
S3	94891571.07	94891569.37	1.79282E-06
S6	95226681.16	95226672.68	8.90565E-06
S9	93732369.76	93732355.78	1.49133E-05
S11	99341937.74	99341954.77	-1.7146E-05
S14	84488597.49	84488598.86	-1.6179E-06
S18	92258348.37	92258334.55	1.49742E-05
S19	90801131.26	90801129.25	2.21219E-06
S22	84576547.59	84576561.21	-1.611E-05

$$L_2 = \frac{f_2}{c} \left[ L_1 \frac{c}{f_1} - \left( \frac{1}{f_2^2} - \frac{1}{f_1^2} \right) \cdot \alpha \cdot TEC_L \right]$$

Table 3 shows the estimated values, the actual values of L2 and the difference between them for each satellite, where the differences indicated an agreement between the model-derived estimates and the direct measurements at the level of -1.6179E-06%.

Shown in Table 3 are the difference error estimates in percentage calculated using the following equation:

$$DE = \frac{L_{2\text{calculated}} - L_{2\text{actual}}}{L_{2\text{calculated}}} \cdot 100$$

## 5. Conclusion

The accuracy of single-frequency data benefits from calibration of the total electron content (TEC) of the ionosphere below the satellite. Data from a global network of global positioning system (GPS) receivers provides timely, continuous, and globally well-distributed measurements of ionospheric electron content.

Typically, one does not know the actual refractive index profile at a particular location, so prediction models are often used to account for neutral atmosphere delay.

Based on the experimental results obtained so far, the following conclusions can be drawn:

- An alternative methodology has been proposed to estimate the TEC at any GPS station from spread GPS station around the concerned station.
- The experimental results indicate that the difference between estimated TEC and the actual TEC for satellite # S14 reached to 0.00237%.
- An alternative methodology has been proposed to predict the value of L2 at any GPS station from spread GPS station around the concerned station.

- The experimental results indicate that the difference between predicted value of L2 and the actual value of L2 for satellite # S14 reached to 1.6179E-06%.
- It has been shown that the coordinated analysis of GPS derived TEC maps can contribute to improve positioning by GPS.
- This TEC map shows that well and equal spaced contour line due to strong correlation between TEC values for all GPS stations.
- Daily estimates of GPS coordinates are temporally correlated and it is therefore incorrect to assume that the observations are independent when estimating parameters from them.

## References

- [1] P. Zhong et al., Adaptive wavelet transform based on cross-validation method and its application to GPS multipath mitigation, *GPS Solution* 12 (2008) 109–117.
- [2] L. Lin, Remote sensing of Ionosphere using GPS measurements, 22<sup>nd</sup> Asian conference on remote sensing, 5–9 November 2001, Singapore.
- [3] A. Indriyatmoko, Artificial neural networks for predicting DGPS carrier phase and pseudorange correction, *GPS Solution* 12 (2008) 237–247.
- [4] Y. Gao, Precise Ionosphere Modeling Using Regional GPS Network Data, *Journal of Global Positioning Systems* 1 (1) (2002) 18–24.
- [5] <http://en.wikipedia.org/wiki/ionosphere>.
- [6] F. Rodrigo et al., UNB3m\_pack: a neutral atmosphere delay package for radiometric space techniques, *GPS Solution* 12 (2008) 65–70.
- [7] F. Rodrigo et al., Development of a regional GPS-based ionospheric TEC model for South Africa, *Advances in Space Research* 39 (2007) 808–815.
- [8] Xu. Guochang, *GPS Theory, Algorithms and Applications*, © Springer-Verlag Berlin Heidelberg 2003, 2007.

- [9] Julian A.R. Rose, The use of ionospheric tomography and elevation masks to reduce the overall error in single-frequency GPS timing applications, *Advances in Space Research* (2010).
- [10] B.A. Iijima, Automated daily process for global ionospheric total electron content maps and satellite ocean altimeter ionospheric calibration based on Global Positioning System data, *Journal of Atmospheric and Solar-Terrestrial Physics* 61 (1999) 1205–1218.